2009

Tomato Bushy Stunt Virus (TBSV), A Versatile Platform for Polyvalent Display of Antigenic Epitopes and Vaccine Design

Shantanu Kumar
Department of Molecular Biology, TPC-6, The Scripps Research Institute, 10550 North Torrey Pines Road, La Jolla, CA 92037, USA

Wendy Ochoa
Department of Molecular Biology, TPC-6, The Scripps Research Institute, 10550 North Torrey Pines Road, La Jolla, CA 92037, USA

Pratik Singh
Department of Cell Biology, The Scripps Research Institute, La Jolla, CA 92037, USA

Catherine Hsu
Department of Molecular Biology, TPC-6, The Scripps Research Institute, 10550 North Torrey Pines Road, La Jolla, CA 92037, USA

Anette Schneemann
Department of Molecular Biology, TPC-6, The Scripps Research Institute, 10550 North Torrey Pines Road, La Jolla, CA 92037, USA

See next page for additional authors

Virology 388 (2009) 185–190

Contents lists available at ScienceDirect

Virology

journal homepage: www.elsevier.com/locate/yviro

Tomato bushy stunt virus (TBSV), a versatile platform for polyvalent display of antigenic epitopes and vaccine design

Shantanu Kumar [a], Wendy Ochoa [a], Pratik Singh [b], Catherine Hsu [a], Anette Schneemann [a], Marianne Manchester [b], Mark Olson [c], Vijay Reddy [a,*]

[a] Department of Molecular Biology, TPC-6, The Scripps Research Institute, 10550 North Torrey Pines Road, La Jolla, CA 92037, USA
[b] Department of Cell Biology, The Scripps Research Institute, La Jolla, CA 92037, USA
[c] Department of Cell Biology and Biochemistry, U.S. Army Medical Research Institute of Infectious Diseases (USAMRIID), Frederick, MD 21702, USA

ARTICLE INFO

Article history:
Received 7 January 2009
Returned to author for revision
20 February 2009
Accepted 28 February 2009
Available online 2 April 2009

Keywords:
Virus-like particles
Tomato bushy stunt virus
Capsid display
Vaccine design
Ricin vaccine

ABSTRACT

Viruses-like particles (VLPs) are frequently being used as platforms for polyvalent display of foreign epitopes of interest on their capsid surface to improve their presentation enhancing the antigenicity and host immune response. In the present study, we used the VLPs of Tomato bushy stunt virus (TBSV), an icosahedral plant virus, as a platform to display 180 copies of 16 amino acid epitopes of ricin toxin fused to the C-terminal end of a modified TBSV capsid protein (NΔ52). Expression of the chimeric recombinant protein in insect cells resulted in spontaneous assembly of VLPs displaying the ricin epitope. Cryo-electron microscopy and image reconstruction of the chimeric VLPs at 22 Å resolution revealed the locations and orientation of the ricin epitope exposed on the TBSV capsid surface. Furthermore, injection of chimeric VLPs into mice generated antisera that detected the native ricin toxin. The ease of fusing of short peptides of 15–20 residues and their ability to form two kinds ($T=1$, $T=3$) of bio-nanoparticles that result in the display of 60 or 180 copies of less constrained and highly exposed antigenic epitopes makes TBSV an attractive and versatile display platform for vaccine design.

Introduction

It has been previously described that antigen density greatly influences the magnitude of antibody response (Bachmann et al., 1993; Dintzis et al., 1976; Milich et al., 1997). High-density of antigens can be achieved by attaching antigenic epitopes to the viral coat protein (CP) subunits, thus generating virus-like particles (VLPs) that display the chosen epitopes. Virus capsids in general are natural multivalent assemblies composed of multiple copies, ranging from 60 to 1000s, of one or few kinds of CPs. A variety of VLPs from diverse sources are being used as polyvalent display platforms (Manchester and Singh, 2006). VLPs displaying epitopes of interest on their external surfaces are being explored as candidate vaccines and/or as therapeutics agents against microbial diseases (Jegerlehner et al., 2002; Khor et al., 2002; Ludwig and Wagner, 2007; Manayani et al., 2007; Peabody et al., 2008; Shivachandra et al., 2007).

A number of simple viruses such as cowpea mosaic virus (CPMV), Flock House virus (FHV) and bacteriophage MS2 have been utilized to display peptides of interest on the viral surfaces by inserting them into exposed loops of the respective CP subunits (Khor et al., 2002; Manayani et al., 2007; Porta et al., 1994). In addition, complex assemblies like bacteriophage T4 are being use to display foreign molecules of interest (Fokine et al., 2007; Li et al., 2007; Shivachandra et al., 2007). In the case of simple viruses such as CPMV and FHV, the inserted epitopes often undergo proteolytic cleavage resulting in unanticipated problems. Unlike these cases, TBSV provides a unique display platform as the peptides of interest could be fused at the end of C-terminus, which is surface exposed and displayed as linear peptides, which are free to adopt one or more of their native conformation(s).

Tomato bushy stunt virus (TBSV) is a spherical plant virus that belongs to the family of Tombusviridae. The three-dimensional structure of TBSV is available at 2.9 Å resolution (Harrison et al., 1978; Olson et al., 1983). The native capsids of TBSV are ~320 Å in diameter and are composed of 180 copies of a single 41 kDa CP subunit arranged with $T=3$ icosahedral symmetry. Tertiary structure of the TBSV-CP subunit consists of 3 domains. The N-terminal R-domain, located at the interior of the capsid, interacts with the encapsidated RNA. This is followed by a shell (S) domain, which forms the contiguous shell of the capsid and a C-terminal protruding (P) domain exposed on the capsid exterior (Fig. 1). In the case of TBSV, the display of foreign epitopes is accomplished by genetically appending the peptides of interest to the C-terminus of the CP, which results in the display of peptides on the capsid surface. This was earlier demonstrated by generating the chimeric capsids of TBSV, expressed in

* Corresponding author. Fax: +1 858 784 8896.
E-mail address: reddyv@scripps.edu (V. Reddy).

0042-6822/$ – see front matter © 2009 Elsevier Inc. All rights reserved.
doi:10.1016/j.virol.2009.02.051

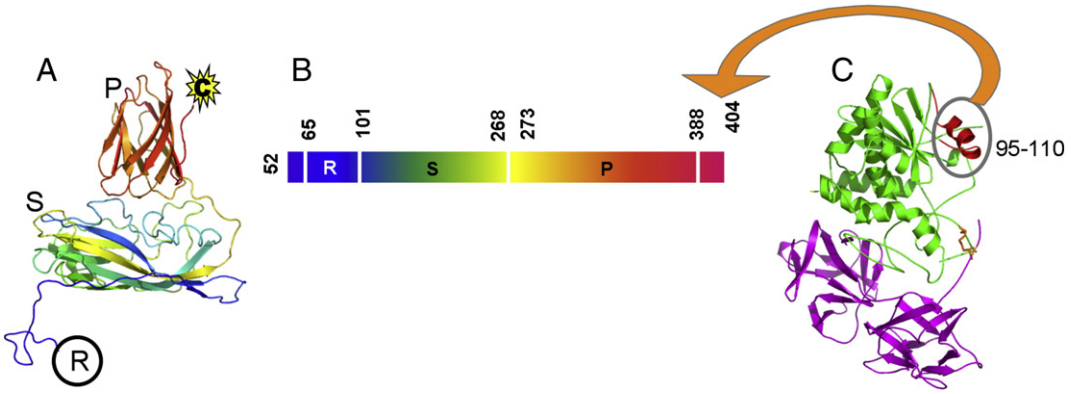

Fig. 1. Schematic presentation of fusion between NΔ52-TBSV capsid protein and 16 amino acid ricin epitopes. (A) Tertiary structure and organization of the individual domains R, S and P of the TBSV coat protein subunit (B) Schematic presentation of the fusion of 16 a.a. ricin epitope to the C-terminus of TBSV capsid protein. (C) Tertiary structure of the ricin toxin and the location of 16 amino acid ricin epitopes (red) fused to TBSV-CP. A and B-chains of the ricin toxin are shown in green and magenta, respectively.

plants, by displaying a short peptide of 13 a.a. from GP120 of HIV (Joelson et al., 1997).

The overall goal of this study was to generate a potential vaccine for ricin toxin, which remains a common bio-terrorism agent. We report here successful generation of $T=3$ chimeric capsids (VLPs) of TBSV, in insect cells using a baculovirus expression system, displaying 180 copies of a 16 a.a. epitope from the ricin toxin A-chain (RTA) and their efficacy in eliciting immune response in mice against the ricin toxin. Furthermore, Cryo-electron microscopy reconstruction of the chimeric particles of TBSV-RTA peptide revealed the locations and their relative orientation (presentation) of the ricin peptide(s) on the capsid surface of TBSV.

Results

Fusion of ricin epitope to the C-terminus of TBSV capsid protein and assembly of chimeric TBSV-RTA VLPs

Cloning and expression of N-terminal deletion mutants of TBSV have been described previously (Hsu et al., 2006). One of the deletion mutants, NΔ52-TBSV, which lacks the N-terminal 52 amino acids of the TBSV coat protein (CP) yet efficiently forms $T=3$ particles (Hsu et al., 2006) was sub-cloned and fused with a 16 amino acid epitope (residues 95–110) of the ricin toxin A-chain (RTA) at the C-terminus (Fig. 1). The crystal structure of TBSV clearly indicated that the C-terminus of TBSV is free and exposed on the capsid surface (Harrison et al., 1978; Olson et al., 1983). Hence, fusion of the peptide of interest at the C-terminal end allows the display of the peptide on the outer capsid surface. Using homologous recombination with linearized baculovirus genome, a recombinant baculovirus (VSR-20) was generated, which resulted in the expression of the chimeric protein, TBSV-RTA16 (TBSV-NΔ52-16 a.a. ricin epitope) and assembly of virus like particles (VLPs). The chimeric (VLPs) expressing ricin epitope were purified by pelleting the particles onto 30% sucrose cushion and further purified on 10–40% sucrose gradients. The purified TBSV-RTA16 VLPs were analyzed on a 10% Tris–glycine SDS-PAGE, which showed a single band of approximately 37 kDa protein (Fig. 2A, lane 2). Western blot analysis of TBSV-NΔ72 (a 72 residue N-terminal deletion mutant of TBSV-CP) and TBSV-RTA16 VLPs was performed with antibodies raised against denatured TBSV-CP or polyclonal antibodies raised against ricin toxin. The TBSV-NΔ72 as well as the TBSV-RTA16 proteins were recognized by the antisera against the TBSV-CP (Fig. 2B). Both the monomers and dimers of TBSV-NΔ72 and TBSV-RTA16 CPs were detected strongly, whereas unresolved oligomers of TBSV-CPs were seen as a smear at the top of the blot (Fig 2B, lanes 1&2). It is interesting to note that the TBSV-CP was detected in

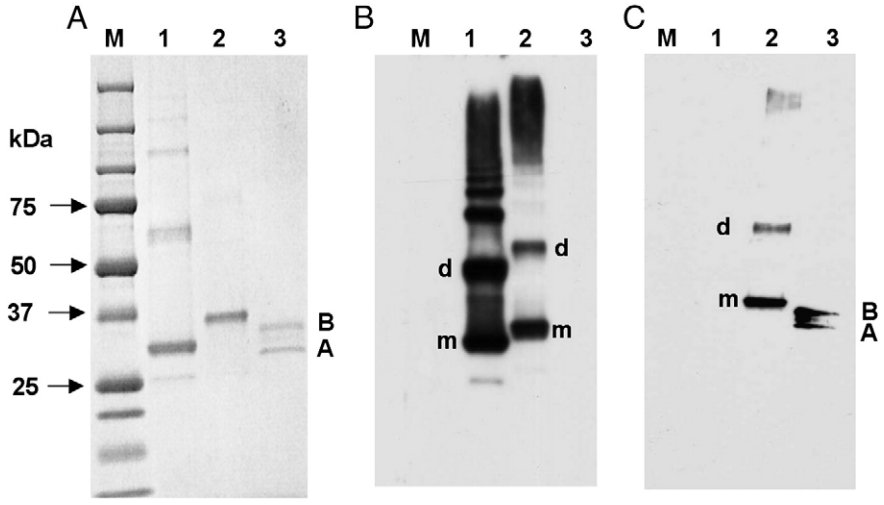

Fig. 2. Expression of the TBSV-RTA16 coat protein confirmed using SDS-PAGE and Western blot analysis. (A) SDS-PAGE analysis of the NΔ72-TBSV protein, chimeric TBSV-RTA16 and ricin toxin, lane M: Molecular weight markers, lane 1: NΔ72-TBSV protein, lane 2: TBSV-RTA16, lane 3: ricin toxin consists of A and B-chains. (B) Western blot analysis using polyclonal antisera due to full length TBSV-CP. Description of the lanes is same as in panel A. Monomers and dimers of the TBSV-CPs are identified as 'm' and 'd' respectively. The smear at the top of the lanes corresponds to unidentified oligomers of the TBSV-CPs. (C) Western blot analysis using polyclonal antisera against ricin toxin. Description of the lanes is same as in panel A. Ricin toxin exists as a hetero-dimer of the A and B-chains.

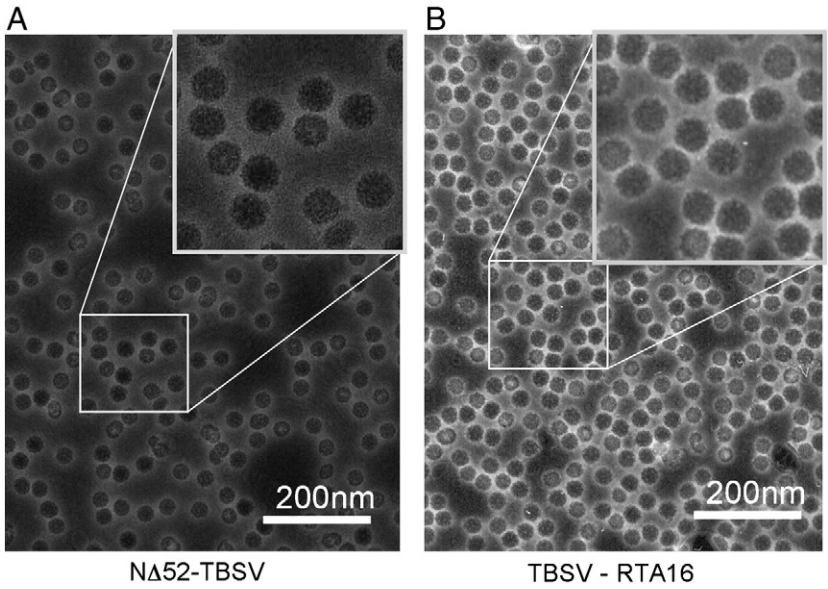

Fig. 3. Transmission electron micrographs of VLPs of TBSV stained using 1% uranyl acetate (A) NΔ52-TBSV and TBSV-RTA16 VLPs (B). Both kinds of VLPs form approximately similar size of VLPs (~35 nm in diameter). Insets show the integrity of VLPs at a higher magnification.

the Western blots by the antibodies raised against denatured CP but not the assembled virions. Similar findings have been reported in previous studies (Joelson et al., 1997). Additionally, the polyclonal ricin antibody detected monomer and dimer forms of TBSV-RTA16 and the A and B-chains of ricin toxin (Fig. 2C, lanes 2&3) suggesting that the RTA epitopes are attached to the TBSV-CP upon formation of chimeric VLPs. It has been shown that the VLPs of TBSV expressed in the insect cells package cellular RNA suggesting the requirement of nucleic acid in the formation for TBSV particles (Hsu et al., 2006). Similar findings have been reported in the case of assembly of analogous particles of TCV (Stockley et al., 1986). Visualization of VLPs of TBSV-RTA16 using transmission electron microscopy and negative staining revealed the presence of homogenous population of particles similar to that of the parent NΔ52-TBSV particles (Fig. 3).

Cryo-electron microscopic reconstruction of TBSV-TRA VLPs

Cryo-electron microscopy and image reconstruction approach was employed to identify the location and relative arrangement of the ricin epitopes on the surface of TBSV. The reconstruction of TBSV-RTA16 particles at 22 Å resolution confirmed the $T=3$ icosahedral arrangement of the chimeric TBSV subunits. The difference maps between the TBSV-RTA16 reconstruction (maps) and the atomic model of the TBSV capsid fitted into the EM density and filtered at 22 Å revealed the location of the ricin epitope displayed at the C-terminus of the TBSV-CP subunit (Fig. 4). Interestingly, the minimum separation of ~32 Å is found between the two adjacent epitopes that come from the icosahedral 2-fold related and quasi 2-fold related C (C2) and A (A5)-subunits, respectively (Fig. 4B). The epitopes on A-

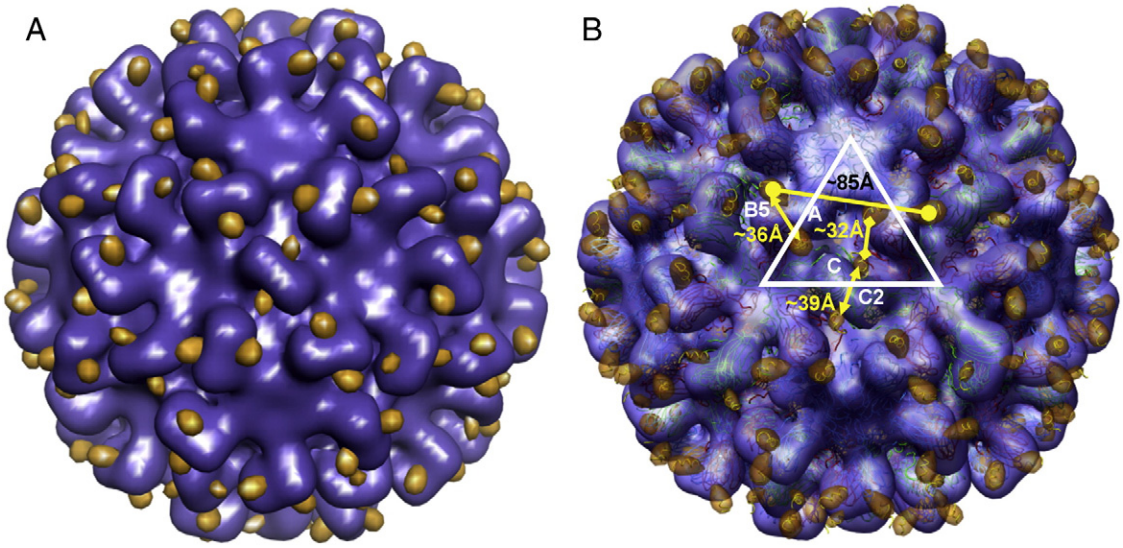

Fig. 4. Cryo-electron microscopy and image reconstruction of TBSV-RTA16 at 22 Å resolution. (A) The electron density of TBSV-CPs is shown in steel blue and the density corresponding to the ricin peptide is shown in gold. (B) An illustration highlighting the quality of fit of atomic structures of the TBSV-CP and the ricin epitope to the electron density, which is shown as a transparent surface. Individual epitopes are exposed with a minimum separation of ~32 Å between two adjacent epitopes, identified by the line with diamonds at the end, which belong to icosahedral 2-fold related and quasi 2-fold related C and A-subunits respectively. The epitopes of AB(5) and CC(2) dimers are separated by 36 Å and 39 Å respectively and identified by the lines with arrows, whereas the epitopes of the A, B and C subunits that constitute the reference icosahedral asymmetric unit are separated by ~85 Å, identified with the line with spheres at the end. The central triangle (white lines) identifies the icosahedral asymmetric unit. Images were generated using the molecular graphics program Chimera (Pettersen et al., 2004).

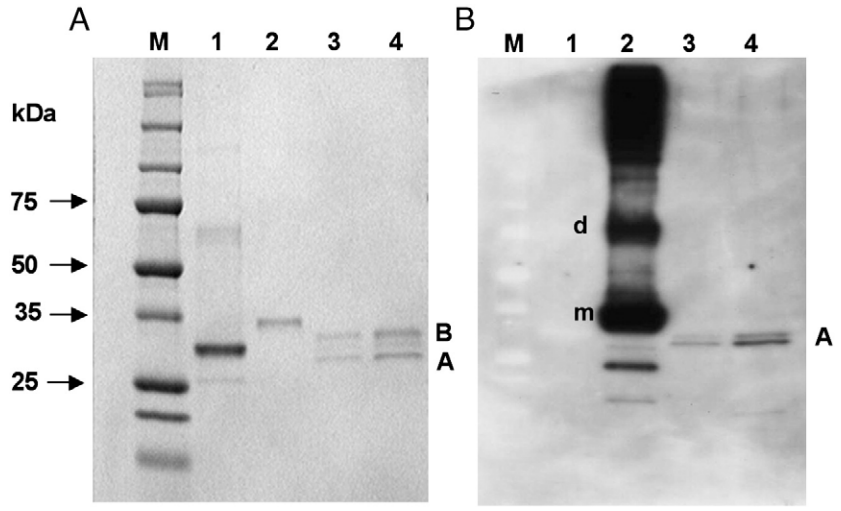

Fig. 5. Detection of TBSV-RTA16 and ricin toxin using the antisera against TBSV-RTA16 VLPs. (A) SDS-PAGE analysis of the TBSV-CPs and ricin toxin, lane M: Molecular weight markers, lane 1: NΔ72-TBSV protein, lane 2: TBSV-RTA16, lane 3: 25 ng of ricin and lane 4: 50 ng of ricin. (B) Western blot analysis using polyclonal antisera raised against TBSV-RTA16. Description of the lanes is same as in the panel A. Monomer and dimer forms of TBSV are indicated as 'm' and 'd' respectively. The A and B-chains of the ricin toxin are identified accordingly. Only the ricin A-chain is detected in the Western blot analysis, as the displayed (fused) ricin epitope belongs to the A-chain.

B5 and C-C2 subunit dimers are separated by ~36 Å and ~39 Å respectively, whereas the epitopes of the A, B and C subunits that constitute the reference icosahedral asymmetric unit are separated by ~85 Å (Fig. 4B).

Immune response against chimeric TBSV-RTA VLPs

The ability of TBSV-RTA16 VLPs to elicit a specific immune response was evaluated by injecting them into mice. BALB/c mice were injected with 20 μg of TBSV-RTA VLPs and boosted once after a week. Sera collected from the mice after 1 week of the second injection and titer (~10^4) was calculated by ELISA (data not shown). In the Western blot analysis, 25–50 ng of ricin chain-A was readily detected (Fig. 5B lanes 3–4) by the anti-sera raised against TBSV-RTA16, demonstrating that the ricin chain-A specific immune response was elicited by the TBSV-RTA16 VLPs. Anti-sera of TBSV-RTA16 was able to detect TBSV-RTA16 (Fig. 5B, lane 2) but not the TBSV-CP (Fig. 5B, lane 1). As noted earlier, the anti-sera raised against the assembled TBSV capsids did not detect the denatured protein, suggesting that the anti-sera of TBSV-RTA16 are in fact detecting the ricin epitope in the blot (Fig. 5B, lane 2).

Discussion

In the present study we have demonstrated the display of 180 copies of the 16 a.a. epitope from the ricin A-chain on the surface of the TBSV capsid by attaching the peptide to the C-terminus of TBSV subunit. The VLPs produced using the recombinant baculovirus system were very stable and could be purified in large quantities. The assembly of TBSV-RTA16 particles was not affected by the addition of 16 a.a. peptide at the C-terminus. Cryo-electron microscopy and image reconstruction of the recombinant VLPs clearly indicated that the displayed copies of the ricin epitope are highly exposed on the capsid surface and clearly separated from one another (Fig. 4). Importantly, the TBSV-RTA16 particles elicited a strong immune response against ricin epitope when the chimeric VLPs were injected into mice.

Morris and coworkers (Joelson et al., 1997) reported earlier the display of a 13 a.a. epitope from GP120 of HIV-1 on the surface of TBSV by fusing the peptide at the carboxy-end of the TBSV subunit. These particles were generated in plants and package a full complement of the entire viral genome, hence are infectious. In the present study, even though the particles generated in insect cells contain cellular RNA, it has been shown that there is no full length viral mRNA present in these particles, thus preventing viral replication (Hsu et al., 2006).

Unlike other VLPs of CPMV, FHV and MS2, where the epitopes are inserted into loops, TBSV provides a unique display platform as the peptides of interest could be attached to the C-terminus of the TBSV-CP that allows the display of the epitopes as linear peptides on the capsid surface. This in turn allows the epitopes to freely adopt their one or more native conformations. Furthermore, specific TBSV-CP subunits (e.g., TBSV-NΔ52, TBSV-NΔ62 or TBSV-NΔ72) can be selected to generate bio-nanoparticles of appropriate size, $T=1$ particles of 200 Å in diameter vs. $T=3$ particles of 350 Å in diameter, displaying either 60 or 180 copies of epitopes respectively. Together with the ease of genetically fusing the epitopes of interest to the C-terminus of the CP makes TBSV a versatile platform for displaying antigenic epitopes. Polyvalent display of antigens has been proven to be very effective in eliciting immune response against peptides of interest (Chackerian et al., 1999, 2008). Thus, the recombinant TBSV-VLPs could potentially be used as a vaccine platform for various antigens of interest from variety of pathogens because there would be no pre-existing immunity against TBSV in animals and humans. We are in the process of undertaking ricin toxicity challenge experiments in mice to assess the efficacy of TBSV based polyvalent reagents. Furthermore, evaluation of scope and possibility of displaying larger peptides between 30–200 residues is underway.

Materials and methods

Cell culture

Insect cells, *Spodoptera frugiperda*, (line IPLB-*Sf21*) were grown in TC100 medium (Invitrogen, Carlsbad, CA) at 27 °C. Growth media was supplemented with 0.35 g of $NaHCO_3$ per liter 2.6 g of tryptose broth per liter, 2 mM L-glutamine, 100 U of penicillin and streptomycin per mL and 10% heat-inactivated fetal bovine serum. Cultures were maintained as monolayer in screw-capped plastic flasks or as suspensions in 1-liter spinner flasks.

Generation of recombinant baculoviruses expressing TBSV-RTA fusion protein

The cDNA clone of TBSV-CP in plasmid pTCTBcp was a generous gift from Drs. T.J. Morris and F. Qu (University of Nebraska, Lincoln, Nebraska). N-terminal deletion mutants of TBSV capsid proteins

(NΔ52-TBSV, NΔ62-TBSV, NΔ72-TBSV) have been described in detailed (Hsu et al., 2006). In order to generate chimeric DNA molecules of NΔ52TBSV-RTA16, the mutant TBSV-CP (NΔ52-TBSV) sequence and ricin epitope (95–110 amino acids) was PCR amplified and fused using a standard mutagenic PCR technique (Ho et al., 1989). Chimeric DNA fragment (NΔ52TBSV-RTA16) was cloned in a TOPO T/A cloning vector (Invitrogen, CA) and later sequenced to confirm the accuracy as well as fusion of TBSV and RTA fragment. To facilitate cloning of chimeric DNA fragment into the multiple cloning site of pBacPAK9, BamHI and XhoI restriction site sequences were added to the 5′ and 3′ ends of the NΔ52TBSV-RTA16, respectively and cloned into a baculovirus transfer vector, pBacPAK9 (Clontech, CA) and named as VSR15. All the PCR reaction was performed using Platinum Pfx DNA polymerase (Invitrogen, CA). Recombinant baculoviruses expressing NΔ52TBSV-RTA16 was generated by co-transfecting VSR15 plasmid constructs with linearized baculovirus DNA into Sf21 insect cells according to the manufacturer's instructions (Clontech, CA). Recombinant baculovirus expressing Δ52TBSV-RTA16 was named as VSR20 and was plaque purified twice and further amplified to obtain pure stocks with high viral titers.

Protein expression, purification and SDS-PAGE analysis

Sf-21 cells were plated at a density of 8×10^6 cells per 10 cm tissue culture dish and were infected with stocks of VSR20 with an MOI of 5 per cell. Cells and supernatant were harvested 72 h post infection. Nonidet P-40 was added to a final concentration of 1% (v/v) and incubated on ice for 10 min to lyse the cells. Cell debris was pelleted by centrifugation at $13,800\times g$ for 10 min at 4 °C in a JA17 rotor (Beckman, Fullerton, CA). The VLPs in the supernatant were pelleted through a 30% sucrose (wt/wt) cushion by ultracentrifugation at $184,048\times g$ for 2.5 h in a 50.2 Ti rotor (Beckman) at 4 °C. Pellets were then resuspended in sodium acetate buffer (100 mM Sodium Acetate, 50 mM NaCl, 10 mM $CaCl_2$ and pH 5.5) overnight at 4 °C. Insoluble material in the resuspended pellet was removed by centrifugation at $12,000\times g$ for 10 min in a micro-centrifuge. To further purify VLPs, the supernatant was loaded onto 10–40% sucrose gradients (wt/wt) made in sodium acetate buffer and centrifuged at $197,500\times g$ for 2 h in a SW-41 rotor (Beckman). VLPs were harvested from gradients by puncturing the sides of the tubes with a needle and aspirating the bands using a syringe or by ISCO gradient fractionator (Teledyne, Los Angeles, CA) at 0.75 mL/min and 0.5 min per fraction. Purified VLPs were dialyzed in sodium acetate buffer overnight at 4 °C. The VLPs were concentrated using Amicon ultra having molecular cut off 100 kDa (Millipore, USA). Purified VLPs of TBSV-RTA16, NΔ72-TBSV and purified ricin (positive control for ricin) were resolved on the 10% Tris–glycin gel (Invitrogen, CA) and stained with simple blue using manufacturer's instructions (Invitrogen, CA). Gels were documented using Alpha Imager® gel documentation system (Alpha Innotech, USA).

Production of hyperimmune antiserum against TBSV-RTA16 and ELISA

To produce hyperimmune serum, mice were immunized with recombinant TBSV-RTA16 VLPs. The immunization regimen consisted of one intramuscular injection of the purified CP of TBSV-RTA16 in Freund's adjuvant (at a dose of 60 μg per mouse) followed by one booster injection of the same dose in Freund's incomplete adjuvant. The animals were bled 1 week after the last booster injection. An enzyme-linked immunosorbent assay (ELISA) was performed to quantify the titer of antibody. Briefly, the VLPs were directly applied to microplates (Nun-immuno plates) at 100 μl per well and a final concentration of 1 μg/mL in carbonate–bicarbonate buffer (0.05 M, pH 9.6) and were incubated overnight at 4 °C. The antigen-coated plates were blocked for 2 h at room temperature with 5% nonfat milk in 0.01 M phosphate-buffered saline (PBS) (pH 7.2) and washed thrice with PBS containing 0.05% Tween 20 (PBST). Different dilutions of primary antisera (1:10, 1:100, 1:1,000, and 1:10,000) were incubated with the antigen for 1 h at room temperature and washed thrice with PBST. Anti-mouse immunoglobulin (Sigma) was diluted 1:10,000, and the plates were incubated for 1 h at room temperature. Following incubation, the plates were washed thrice with PBST, 3,3′,5,5′-tetramethyl benzidine (TMB)-peroxidase substrate (Sigma) was added, and the color was allowed to develop for 10 min at room temperature. The reaction was stopped by adding 1% SDS, and the optical density at 405 nm was determined with a Spectra Max-250 (Molecular Devices, CA).

Immuno detection of TBSV-RTA16

Protein concentration of purified VLPs of TBSV-RTA16, NΔ72-TBSV and purified ricin (positive control for ricin) was estimated using BCA protein assay reagent (Pierce, USA) according to the manufacturer's instructions. One microgram of protein sample (1 mg/mL) was diluted in 2× SDS loading buffer (250 mM Tris, pH 6.8, 2% (w/v) SDS, 10% (v/v) glycerol, 100 mM dithiothreitol (DTT), and 0.1% (w/v) bromophenol blue) and boiled for 2 min. SDS-PAGE was performed using 10% Tris–glycin gel (Invitrogen, CA). After completion of SDS-PAGE, gel was electroblotted to PVDF membrane in transfer buffer (Invitrogen, CA) containing 20% methanol at a constant voltage (30 V) for 2 h. Prestained molecular weight standards (Bio-Rad) were used to monitor protein transfer. Membranes were blocked for 1 h in blocking buffer (5% dried milk, 0.1% Tween 20 in PBS) at room temperature and later incubated at 4 °C overnight in primary antibody against ricin (Vector Labs, Burlingame, CA) or against TBSV-RTA16, diluted (1:1000). Membranes were washed for 30 min with 3 changes of washing buffer (0.1% Tween 20 in PBS), and incubated with HRP-conjugated secondary antibody, diluted (1:5000 in PBS-Tween 20) for an hour. After another 30 min wash, with 3 changes of wash buffer, blot was reacted with SuperSignal chemiluminescent substrates (Pierce, USA). Blot was exposed on Kodak X-ray films for the visualization of protein band.

Electron microscopy

Carbon-coated, copper grids were glow discharged in the presence of amyl acetate immediately before loading samples. Grids were placed in 10 μL of VLP samples for 1 min, washed three times in sterile filtered water and stained in 10 μL drops of 1% uranyl acetate three times allowing the grids to soak in the last drop of stain for 2 min. After drying grids, samples were examined under an electron microscope (Phillips CM100).

Cryo-electron microscopy and image reconstruction

Aliquots of the virus suspension at a concentration of about 2–3 mg/mL were applied to previously glow-discharged Quantifoil EM grids, which were then blotted and plunged into a bath of liquid ethane (−180 °C) using Vitrobot from FEI. The grids were then transferred from liquid nitrogen to a pre-cooled specimen holder (Gatan) that maintained the frozen hydrated sample at −184 °C in a Philips Tecnai F20 FEG transmission cryo-electron microscope operating at 120 kV with a CCD camera. Digital images were recorded under low-dose conditions (~10 e/Å^2) and those that displayed minimal astigmatism and drift as assessed by visual inspection and diffraction were selected for further analysis. Particles clearly separated from neighbors or background contamination were selected and masked as individual images using the software ROBEM (Baker et al., 1999). The image intensity values were adjusted to remove linear background gradients and to normalize the means and variances of the data. The initial orientation and origin parameters of the images for the reconstruction were determined by a model based refinement

approach (Baker et al., 1999). To optimize the search procedure, calculations were performed using only a portion of the Fourier transform of the masked image ($1/70\ Å^{-1}$–$1/30\ Å^{-1}$) to remove both low and high frequency noises. The translation (x,y) and orientation (0,0,w) parameters were refined for each particle by using repeated cycles of correlation procedures (Baker et al., 1988, 1991, 1999; Fuller, 1987). Images were typically discarded if they showed a correlation coefficient calculated between the raw image and the corresponding projected view of an intermediate reconstruction, greater than one standard deviation below the mean coefficient of the entire data set. The final maps were computed based on a total of 342 particles to a resolution of 22 Å. The resolution of the map was estimated by dividing the particle images into two sets, generating two reconstructions and comparing the correlation coefficients and phase residual of the two sets of structure factors as a function of spatial frequency.

Acknowledgments

The authors would like to thank Professor Glen Nemerow and Dr. Sangita Venkataraman for carefully going through the manuscript and for helpful suggestions. The authors are extremely grateful to Drs. Jack Morris and Feng Qu of University of Nebraska, Lincoln, Nebraska for the cDNA clones of TBSV. The authors also like to thank Dr. H.B. Scholthof (Texas A&M University, College Station, TX) for the gift of native TBSV particles. The work reported in this manuscript was fully supported by a contract, W81XWH-04-2-0027 from U.S. Army to V.S.R.

References

Bachmann, M.F., Rohrer, U.H., Kundig, T.M., Burki, K., Hengartner, H., Zinkernagel, R.M., 1993. The influence of antigen organization on B cell responsiveness. Science 262 (5138), 1448–1451.

Baker, T.S., Drak, J., Bina, M., 1988. Reconstruction of the three-dimensional structure of simian virus 40 and visualization of the chromatin core. Proc. Natl. Acad. Sci. U.S.A. 85 (2), 422–426.

Baker, T.S., Newcomb, W.W., Olson, N.H., Cowsert, L.M., Olson, C., Brown, J.C., 1991. Structures of bovine and human papillomaviruses. Analysis by cryoelectron microscopy and three-dimensional image reconstruction. Biophys. J. 60 (6), 1445–1456.

Baker, T.S., Olson, N.H., Fuller, S.D., 1999. Adding the third dimension to virus life cycles: three-dimensional reconstruction of icosahedral viruses from cryo-electron micrographs. Microbiol. Mol. Biol. Rev. 63 (4), 862–922 table of contents.

Chackerian, B., Durfee, M.R., Schiller, J.T., 2008. Virus-like display of a neo-self antigen reverses B cell anergy in a B cell receptor transgenic mouse model. J. Immunol. 180 (9), 5816–5825.

Chackerian, B., Lowy, D.R., Schiller, J.T., 1999. Induction of autoantibodies to mouse CCR5 with recombinant papillomavirus particles. Proc. Natl. Acad. Sci. U.S.A. 96 (5), 2373–2378.

Dintzis, H.M., Dintzis, R.Z., Vogelstein, B., 1976. Molecular determinants of immunogenicity: the immunon model of immune response. Proc. Natl. Acad. Sci. U.S.A. 73 (10), 3671–3675.

Fokine, A., Bowman, V.D., Battisti, A.J., Li, Q., Chipman, P.R., Rao, V.B., Rossmann, M.G., 2007. Cryo-electron microscopy study of bacteriophage T4 displaying anthrax toxin proteins. Virology 367 (2), 422–427.

Fuller, S.D., 1987. The T=4 envelope of Sindbis virus is organized by interactions with a complementary T=3 capsid. Cell 48 (6), 923–934.

Harrison, S.C., Olson, A.J., Schutt, C.E., Winkler, F.K., Bricogne, G., 1978. Tomato bushy stunt virus at 2.9 Å resolution. Nature 276, 368–373.

Ho, S.N., Hunt, H.D., Horton, R.M., Pullen, J.K., Pease, L.R., 1989. Site-directed mutagenesis by overlap extension using the polymerase chain reaction. Gene 77 (1), 51–59.

Hsu, C., Singh, P., Ochoa, W., Manayani, D.J., Manchester, M., Schneemann, A., Reddy, V.S., 2006. Characterization of polymorphism displayed by the coat protein mutants of tomato bushy stunt virus. Virology 349 (1), 222–229.

Jegerlehner, A., Tissot, A., Lechner, F., Sebbel, P., Erdmann, I., Kundig, T., Bachi, T., Storni, T., Jennings, G., Pumpens, P., Renner, W.A., Bachmann, M.F., 2002. A molecular assembly system that renders antigens of choice highly repetitive for induction of protective B cell responses. Vaccine 20 (25–26), 3104–3112.

Joelson, T., Akerblom, L., Oxelfelt, P., Strandberg, B., Tomenius, K., Morris, T.J., 1997. Presentation of a foreign peptide on the surface of tomato bushy stunt virus. J. Gen. Virol. 78 (Pt 6), 1213–1217.

Khor, I.W., Lin, T., Langedijk, J.P., Johnson, J.E., Manchester, M., 2002. Novel strategy for inhibiting viral entry by use of a cellular receptor-plant virus chimera. J. Virol. 76 (9), 4412–4419.

Li, Q., Shivachandra, S.B., Zhang, Z., Rao, V.B., 2007. Assembly of the small outer capsid protein, Soc, on bacteriophage T4: a novel system for high density display of multiple large anthrax toxins and foreign proteins on phage capsid. J. Mol. Biol. 370 (5), 1006–1019.

Ludwig, C., Wagner, R., 2007. Virus-like particles-universal molecular toolboxes. Curr. Opin. Biotechnol. 18 (6), 537–545.

Manayani, D.J., Thomas, D., Dryden, K.A., Reddy, V., Siladi, M.E., Marlett, J.M., Rainey, G.J., Pique, M.E., Scobie, H.M., Yeager, M., Young, J.A., Manchester, M., Schneemann, A., 2007. A viral nanoparticle with dual function as an anthrax antitoxin and vaccine. PLoS Pathog. 3 (10), 1422–1431.

Manchester, M., Singh, P., 2006. Virus-based nanoparticles (VNPs): platform technologies for diagnostic imaging. Adv. Drug Deliv. Rev. 58 (14), 1505–1522.

Milich, D.R., Chen, M., Schodel, F., Peterson, D.L., Jones, J.E., Hughes, J.L., 1997. Role of B cells in antigen presentation of the hepatitis B core. Proc. Natl. Acad. Sci. U.S.A. 94 (26), 14648–14653.

Olson, A.J., Bricogne, G., Harrison, S.C., 1983. Structure of tomato busy stunt virus IV. The virus particle at 2.9 A resolution. J. Mol. Biol. 171 (1), 61–93.

Peabody, D.S., Manifold-Wheeler, B., Medford, A., Jordan, S.K., do Carmo Caldeira, J., Chackerian, B., 2008. Immunogenic display of diverse peptides on virus-like particles of RNA phage MS2. J. Mol. Biol. 380 (1), 252–263.

Pettersen, E.F., Goddard, T.D., Huang, C.C., Couch, G.S., Greenblatt, D.M., Meng, E.C., Ferrin, T.E., 2004. UCSF Chimera—a visualization system for exploratory research and analysis. J. Comput. Chem. 25 (13), 1605–1612.

Porta, C., Spall, V.E., Loveland, J., Johnson, J.E., Barker, P.J., Lomonossoff, G.P., 1994. Development of cowpea mosaic virus as a high-yielding system for the presentation of foreign peptides. Virology 202 (2), 949–955.

Shivachandra, S.B., Li, Q., Peachman, K.K., Matyas, G.R., Leppla, S.H., Alving, C.R., Rao, M., Rao, V.B., 2007. Multicomponent anthrax toxin display and delivery using bacteriophage T4. Vaccine 25 (7), 1225–1235.

Stockley, P.G., Kirsh, A.L., Chow, E.P., Smart, J.E., Harrison, S.C., 1986. Structure of turnip crinkle virus. III. Identification of a unique coat protein dimer. J. Mol. Biol. 191 (4), 721–725.